Osteoblast proliferation on hydroxyapatite coated substrates prepared by right angle magnetron sputtering

Zhendong Hong,[1] Alexandre Mello,[2] Tomohiko Yoshida,[3] Lan Luan,[1] Paula H. Stern,[3] Alexandre Rossi,[2] Don E. Ellis,[1,4] John B. Ketterson[1,5]

[1]*Department of Physics and Astronomy, Northwestern University, Evanston, Illinois 60208*
[2]*Centro Brasileiro de Pesquisas Fisicas, Rio de Janeiro, RJ 22290, Brasil*
[3]*Department of Molecular Pharmacology and Biological Chemistry, Feinberg School of Medicine, Northwestern University, Chicago, Illinois 60611*
[4]*Department of Chemistry, Northwestern University, Evanston, Illinois 60208*
[5]*Department of Electrical and Computer Engineering, Northwestern University, Evanston, Illinois 60208*

Received 28 May 2008; revised 20 January 2009; accepted 27 January 2009
Published online 24 August 2009 in Wiley InterScience (www.interscience.wiley.com). DOI: 10.1002/jbm.a.32556

Abstract: The preparation of hydroxyapatite (HA) coatings via a versatile right-angle magnetron sputtering (RAMS) approach for use as a biomaterial has recently been reported. RAMS coatings show some advantages over conventionally sputtered films in that room temperature deposition yields nanocrystalline and nearly stoichiometric HA coatings under appropriate conditions, thereby avoiding the troublesome post deposition annealing treatment. In this article, we present an exploratory study of the biocompatibility of RAMS HA coatings deposited on metallic substrates. RAMS HA coatings with a thickness around 500nm were prepared on various substrates. X-ray diffraction (XRD) analysis showed that the as-deposited HA coatings were polycrystalline with some strongly preferred orientations. Atomic force microscopy (AFM) results showed that the coatings were rather smooth with surface roughness on the order of 10 nm. X-ray photoelectron spectroscopy (XPS) confirmed that the surface chemistry was nearly stoichiometric. To study the biocompatibility of these coatings, murine pre-osteoblastic MC3T3-E1 cells were seeded onto various substrates. Cell density counts using fluorescence microscopy showed that the best osteoblast proliferation is achieved on an HA RAMS-coated titanium substrate. Additionally, in preliminary studies the influence of Zn, Mg, and Al incorporation in the HA crystal lattice on the *in vitro* behavior was also evaluated. These experiments demonstrate that RAMS is a promising coating technique for biomedical applications. © 2009 Wiley Periodicals, Inc. J Biomed Mater Res 93A: 878–885, 2010

Key words: hydroxyapatite; biomaterial; osteoblast; attachment; proliferation

INTRODUCTION

Owing to its inherent biocompatibility, synthetic Hydroxyapatite (HA) forms a strong bond with human bone and is thus a widely used implant material. HA coatings also enhance the cell response of surrounding bone tissue to a metallic or ceramic implant. The rapidly increasing popularity of HA coatings is due to accumulating evidence that an implant coated with a material chemically similar to natural bone should result in a more desirable tissue response. Since ceramic HA is brittle, and thus not suitable for load-bearing applications, HA coatings are applied to dental and medical implant materials to combine the superior mechanical properties of the implant metals with the biocompatibility of HA.[1,2]

To be most effective, HA coatings should remain on the implant metal surface and stimulate bone ingrowth until sufficient bone regenerates at the implant-bone interface. Unfortunately, both the presence of additional phases (other than HA) or a high concentration of an amorphous HA phase in the coating can cause excessive dissolution in a physiological environment and consequently reduce the coating integrity of the implants.[3,4] To decrease the solubility of as-sputtered HA coatings the crystallin-

Correspondence to: Z. Hong; e-mail: z.hong.nu@gmail.com
Contract grant sponsor: U.S. National Science Foundation; contract grant number: DMR-0303491
Contract grant sponsor: Materials Research Center, Northwestern University (MRSEC program); contract grant number: NSF DMR-0076097
Contract grant sponsor: CNPq, Brazil

ity needs to be enhanced,[5] historically making post-deposition annealing a requirement. However, annealing is time consuming, and, more important, is detrimental to the thermo-stability of the underlying implant metal and is often the main cause of crack formation and the degradation in adhesion of the coating to the substrate. Therefore the challenge has been to develop an approach capable of producing phase-pure, highly crystalline HA coatings on various implant materials.

Currently the commercial technique most utilized to deposit HA is plasma spraying. Although this technique has a high deposition rate, there are some disadvantages such as a nonstoichiometric coating, poor adhesion, and relatively low crystallinity.[6,7] Previous studies have demonstrated that HA coatings made by conventional radio frequency (RF) magnetron sputtering show good biological behavior.[8,9] Almost all groups have reported that the as-sputtered HA coatings are amorphous.[10–16] Although a few groups reported the formation of polycrystalline HA when sputtered at high power, the deposition process is usually accompanied by the decomposition of HA into other calcium phosphate phases (such as β-tricalcium phosphate and tetracalcium phosphate).[17]

In vitro experiments on HA coatings prepared by different techniques to study the short-term adhesion and long-term proliferation and differentiation of osteoblastic cells have been discussed in several papers. However, some controversy exists as to (i) whether HA coatings support adhesion and proliferation when compared with bare titanium or glass substrates[18–21]; and (ii) whether nanocrystalline HA coatings enhance osteoblast adhesion and proliferation compared to conventional micron-sized HA coatings.[22–24] In explaining why a significantly higher number of osteoblasts adhered to HA rather than to titanium,[15] it was hypothesized that this phenomenon was caused by the mediation of higher amounts of fibronectin and vitronectin from serum or peptide (RGD) that adhered to HA rather than the blank titanium substrates.[25,26] In contrast, some controversial reports indicated more attachment on pure titanium than on HA,[27] with similar osteoblast morphology,[28,29] indicating no clinical advantage of HA. Another study[30] reported that crystalline HA provides a better substrate for a different cell line (bone marrow stromal cells, BMSCs) than amorphous HA, when the size effect factor is removed. Many factors may play a role here including coating crystallinity, material chemistry, surface roughness, particle size, etc.

We have previously described a right-angle magnetron sputtering (RAMS) technique to prepare nanocrystalline HA coatings at room temperature on various substrates.[31,32] Since *in vitro* cell growth is very sensitive to surface characteristics, it is important to evaluate the adhesion and proliferation on HA coatings prepared by RAMS. Under suitable conditions we can produce thin as-sputtered HA coatings with desirable stoichiometry and crystallinity. Nanocrystalline HA should be more relevant than micron-sized HA from a biological point of view, due to its structural similarity to biological apatite (50 nm × 25 nm × 4 nm). Furthermore, nanocrystalline HA has been shown to inhibit the growth of some types of cancer cells, while having minimal side effects on normal cells.[33] To evaluate the biocompatibility and osteoconductivity of the RAMS HA coatings, *in vitro* studies using the murine calvarial MC3T3-E1 pre-osteoblastic cell line were performed. The cells were cultured in 12-well polystyrene culture plates containing various substrates. Cell adhesion and proliferation were studied as a function of seeding time.

EXPERIMENTAL METHODS

Substrate preparation, coating deposition, and characterization

The substrates we experimented included (a) quartz substrates; (b) Si001 substrates; (c) pure titanium substrates; (d) phase-pure, nearly stoichiometric, and nanocrystalline sputtered HA coatings; and (e) amorphous Zn, Mg, and Al-substituted sputtered HA coatings, respectively.

All substrates were ultrasonically cleaned with acetone before deposition. In addition, the silicon substrates were etched in 5% hydrofluoric acid for 5 min to remove the surface oxide layer and then rinsed with water, leaving a hydrogen-terminated surface that is stable against oxidation under ambient conditions for a short period of time.

The details of the RAMS sputtering system are reported elsewhere.[31] Hydroxyapatite powder containing 5 wt % of M=Zn, Mg, Al were synthesized from dropwise addition of the $(NH_4)_2HPO_4$ aqueous solution to a solution containing $Ca(NO_3)_2$ and $M(NO_3)_{y=2,3}$, M=Zn, Mg and Al, at 90°C, pH = 9.0.[34] After the addition, the solution was stirred for 4 h at the same temperature. The precipitate was separated by filtration, repeatedly washed with deionized boiling water and dried at 100°C for 24 h. The HA targets (1 inch in diameter) were prepared by hot pressing HA powder followed by sintering at 1100°C for 1 h in the air. Ultra-high purity oxygen was used as the reactive gas component, combined with argon as the sputtering gas. RF power (fixed at a total of 130 watts) was applied to the two opposing targets through an impedance matching network. Gas species in the chamber and their molar ratios were monitored and controlled with the help of a residual gas analyzer. In our experiments the partial pressures of argon and oxygen were set at 5.0 mtorr and 1.0 mtorr, respectively. The deposition time was kept constant at 3 h. After deposition, the coatings were characterized with XRD, AFM, and XPS. A Rigaku ATX-G thin film X-ray diffractometer was used to characterize the coating microstructure.

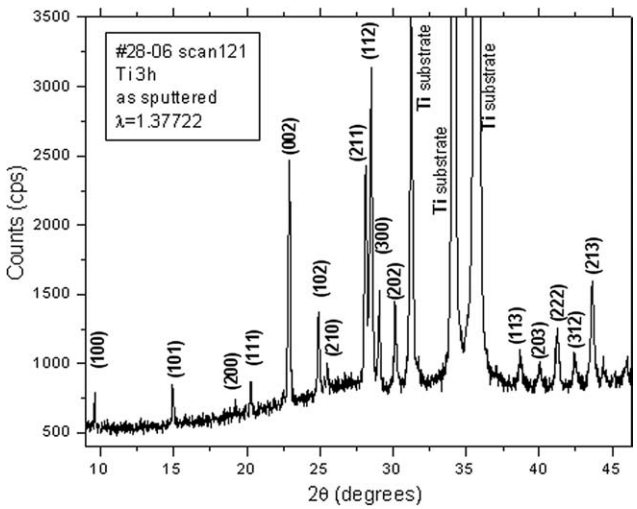

Figure 1. X-ray diffraction pattern of as-sputtered HA coatings on Ti.

Qualitative phase identification was done by comparing the measured XRD intensities with the published International Center for Diffraction Data (ICDD) powder diffraction files. Atomic force microscopy (AFM) images were obtained in the tapping mode with a Digital Instruments (Santa Barbara, CA) Nanoscope atomic force microscope. X-ray Photoelectron Spectroscopy (Omicron ESCAPROBE, Taunusstein, Germany) was used to determine the coating surface composition. All spectra were obtained over the range of 0–1000 eV. The Ca/P ratio was extracted from the ratio of the corresponding integrated peak area after removal of the linear background; the sensitivity factors of the two elements were obtained beforehand by calibrating with powder samples of known composition.

Cell culture

Cell culture media and reagents (α-modified minimum essential medium [α-MEM], penicillin-streptomycin solution, and trypsin/EDTA [0.25% Trypsin with EDTA 4Na]) were obtained from Invitrogen Life Technologies (Carlsbad, CA, USA). Fetal bovine serum (FBS) was purchased from Hyclone (Logan, UT, USA). MC3T3-E1 pre-osteoblastic mouse calvaria-derived cells obtained from RIKEN Cell Bank (Tsukuba, Ibaraki, Japan) were grown in 75 cm^2 Corning cell culture flasks in α-MEM supplemented with 10% FBS and 1% penicillin-streptomycin solution at 37°C under 5% CO_2, and passaged every 7 days. The culture media were changed to fresh media twice a week. After 7 days, cells were sub-cultured using trypsin/EDTA and replated to begin the experiments. Cells at passage numbers 7–23 were used in the experiments without further characterization.

Adhesion and proliferation tests

For the experiments, MC3T3-E1 cells were initially plated at a density of 2,500 cells/well in 50 μL medium directly onto the 1 cm^2 substrates in 12-well Corning/Costar plates, and then cultured at 37°C under 5% CO_2 for 30 min to allow for cell attachment to the substrates. Additional culture medium was then added into each well for a final volume of 1 mL. After 24 h incubation, the culture media were changed to fresh media, and continued to be changed twice a week.

Four hours after seeding the samples were rinsed with phosphate buffered saline (PBS) to remove non-adherent cells, and the adherent cells were fixed with 4% formaldehyde and stained with the Live/Dead Viability/Cytotoxicity Kit (Molecular Probes, OR). The ethidium homodimer stock solution for detecting dead cells is 2 m*M* in DMSO/HOH 1:4(v/v), and diluted in sterile PBS to a final concentration of 2 μ*M*. The calcein-AM stock solution for detecting live cells is 4 m*M* in anhydrous DMSO, and diluted in sterile PBS to a final concentration of 2 μ*M*. All viable cells fluoresced green and all dead/dying cells fluoresced red. The cells were also stained with nuclear stain Hoechst #33342 (Sigma-Aldrich, MO) solution (diluted in sterile PBS to a final concentration of 5 μg/mL) according to manufacturer's instruction for 10 min at room temperature. The cells were then visualized using a Nikon epifluorescence microscope equipped with a UV light source and an accompanying UV filterset. The sample was placed under the microscope and brought into focus. Microscope images were recorded with a Canon G2 digital camera; quantification of cell numbers was achieved with an in-house developed Matlab program using the embedded imaging toolbox

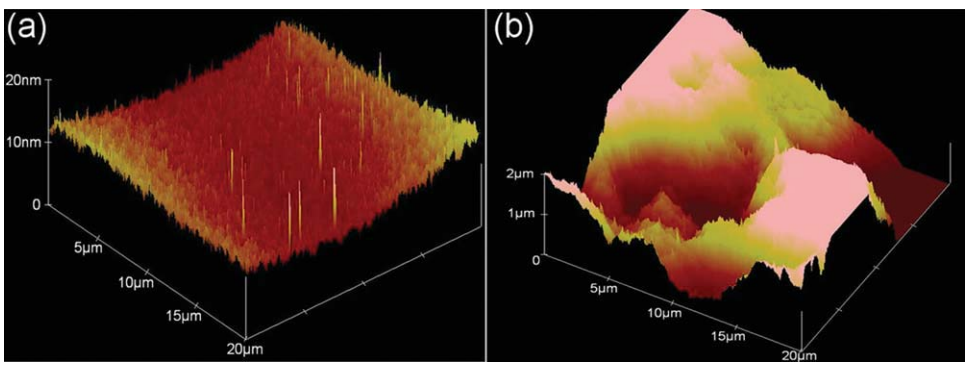

Figure 2. AFM images of as-sputtered HA coatings on (a) Ti/quartz and (b) Ti. [Color figure can be viewed in the online issue, which is available at www.interscience.wiley.com.]

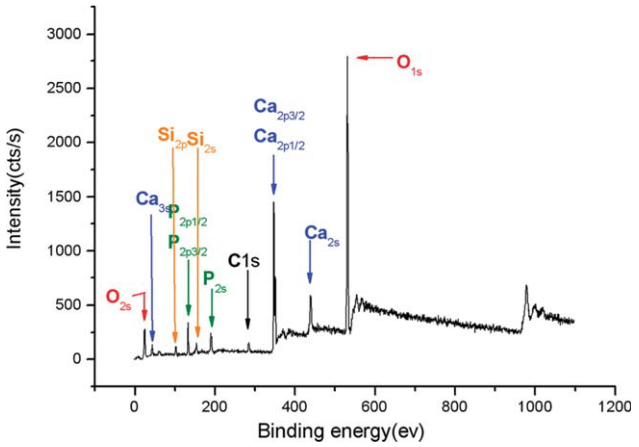

Figure 3. A representative XPS spectrum showing the surface composition of a RAMS HA coating. [Color figure can be viewed in the online issue, which is available at www.interscience.wiley.com.]

functions, and is described elsewhere.[35] Experiments were run in 5 fields per sample and duplicate samples were examined for each condition. Osteoblast adhesion cell density was represented by the mean value along with the standard deviation of each group. Student's *t*-tests were used to evaluate statistical significance, with a p value of 0.1 or less considered statistically significant.

During a 5-day period the cell morphology was observed using light microscopy at 4 h, 1 day, 2 days, and 4 days after seeding. Cell numbers were quantified for each observation and normalized to the initial adhesion to characterize cell proliferation.

RESULTS AND DISCUSSION

Coating characterization

The XRD patterns of HA coated Ti substrates are shown in Figure 1. All HA peaks were identified and the amorphous contribution was very small. The HA peaks have an 0.1° linewidth which is smaller (corresponding to more crystalline material) than HA powder annealed at 1100°C. The mean crystallite size via the Scherer equation ($t = 9{\cdot}\lambda/(B{\cdot}\cos\theta_B)$) is estimated to be within the range of 50 to 100 nm. A post-deposition thermal treatment at 400–600°C did not improve the crystallinity of coatings on Si(001) and Ti substrates but contributed to a preferential orientation along the HA (002) direction.

The film surfaces, on which cells were seeded (Fig. 2), are nearly homogeneous with an rms-roughness of about 10 nm for films grown on titanium/quartz; a considerably larger roughness is seen when titanium substrates are used. In general, the film morphology follows the texture of the substrate surface. The surface chemical composition of HA coatings, determined by XPS spectra, showed the calcium, phosphate and oxygen peaks of only a single mineral species. The Ca/P ratio was observed to be 1.73 ± 0.08, which was close to that for stoichiometric HA (Fig. 3). The carbon peak at 284.8 eV was attributed to hydrocarbon (C—C and C—H bonded carbon) adsorption when the coating was exposed to the atmosphere on removal from the chamber.

Osteoblast adhesion and proliferation

Cell adhesion

Samples tested for osteoblast adhesion included: (A) a quartz substrate, (B) a silicon (001) substrate, (C) a pure titanium substrate, and (D) a titanium substrate coated with HA using RAMS. Importantly, osteoblast adhesion was significantly higher on the RAMS HA coating compared to the other three samples tested (Fig. 4). In contrast, osteoblast adhesion

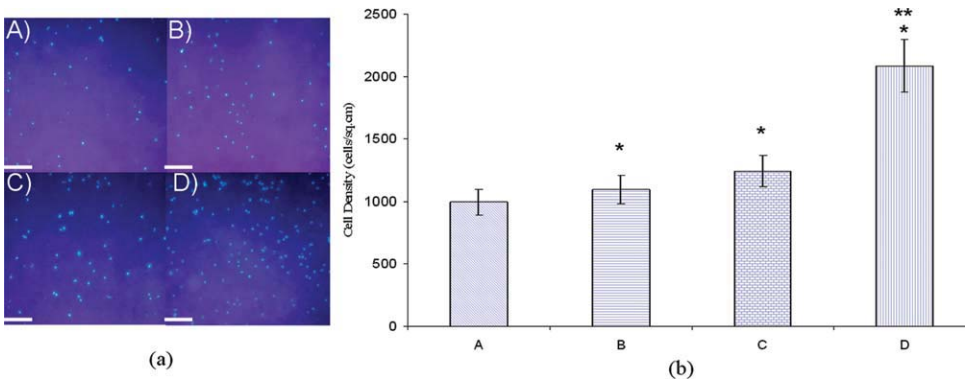

Figure 4. (a) Fluorescence images and (b) osteoblast adhesion on (A) a quartz substrate, (B) a silicon (001) substrate, (C) a blank titanium substrate, and (D) a titanium substrate coated with HA using RAMS. Figure represents mean ± SD. *$p <$ 0.05 compared with the quartz substrate. **$p < 0.1$ compared with blank titanium substrate. Scale bars show 100 μm. [Color figure can be viewed in the online issue, which is available at www.interscience.wiley.com.]

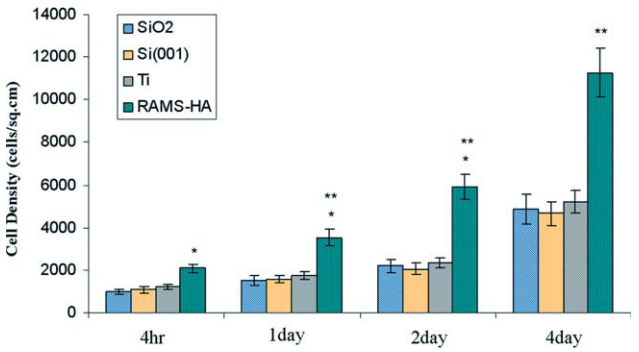

Figure 5. MC3T3-E1 proliferation over the 4-day period. $*p < 0.1$ compared with the quartz substrate. $**p < 0.1$ compared with blank titanium substrate. [Color figure can be viewed in the online issue, which is available at www.interscience.wiley.com.]

was similar among quartz, silicon, and pure titanium. All HA coatings statistically increased osteoblast adhesion above that for uncoated titanium.

It is presumed that such improvements in osteoblast adhesion may be attributed to the surface chemistry and grain size, which are the major difference between the RAMS HA coating and the other three samples tested. The RAMS HA coating has an average grain size of 50–100 nm, compared to several microns for the blank substrates. This translates into increased surface area and more defects/artifacts, which may be an important mechanism to enhance the interaction between osteoblasts and the crystalline coating. Also, the surface of the RAMS coating is bioactive HA and well mimics the natural chemical environment in the bone tissue, which may also be favorable for cell attachment and growth.

Cell proliferation on RAMS HA coatings

Cell proliferation followed a similar trend on all samples tested. Figure 5 shows that the cell number density continues to grow throughout the course of the 4-day experiment on all samples. By day 4, all the samples experienced a 4–5 fold increase in adherent cell numbers. The actual cell numbers may be even greater due to the loss of non-adherent cells during the PBS rinse procedure.

Figure 6 shows the progressive evolution in cell number and cell morphology on a RAMS HA coating obtained by merging light microscopy and fluorescence microcopy images. The spreading of some of the cells was apparent by the first day and the number of cells exhibiting extensions increased over the 4-day period.

Influence of Zn, Mg, and Al substitution

The influence of dopants such as zinc, magnesium, strontium, and aluminum on osteoblast proliferation and differentiation is of interest. Zinc doping of beta-tricalcium phosphate has been reported to have biphasic effect on MC3T3-E1 cell proliferation, with lower concentrations stimulating proliferation, and higher concentrations eliciting inhibitory effects.[35] To address this question with our coatings, hydroxyapatite targets doped with 5 wt % of Zn, Mg, and Al were prepared and used to sputter-coat titanium substrates.

X-ray diffraction analysis (not shown) revealed the surprising result that under the same deposition conditions as those used for pure HA coatings, ZnHA, MgHA, and AlHA coatings all exhibited a highly amorphous nature, i.e., no diffraction peaks other than those from the Ti substrate were found. Clearly the small dopant concentration substituting for calcium altered the microstructure of the sputtered coating in a dramatic way. How zinc, magnesium, and aluminum were incorporated in the HA crystal lattice remains a question.

The MC3T3-E1 osteoblast 4-h adhesion test shows a 20% increase in ZnHA coatings compared with HA, while MgHA behaves comparably to HA; AlHA shows the lowest adhesion (Fig. 7). However at this point it is too early to conclude that this is a universal effect or whether it depends on dosage

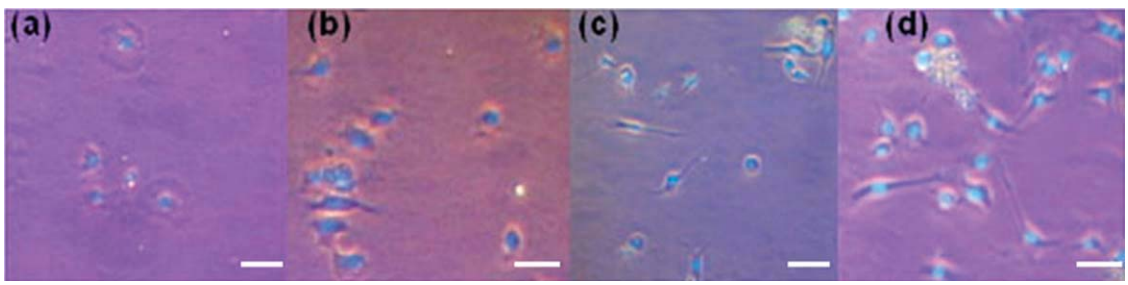

Figure 6. Fluorescence/white-light merged images showing the evolution in cell numbers and morphology with time. (a) $t = 4$ h; (b) $t = 1$ day; (c) $t = 2$ days; (d) $t = 4$ days. The nuclei are stained in blue. Scale bars show 50 μm. [Color figure can be viewed in the online issue, which is available at www.interscience.wiley.com.]

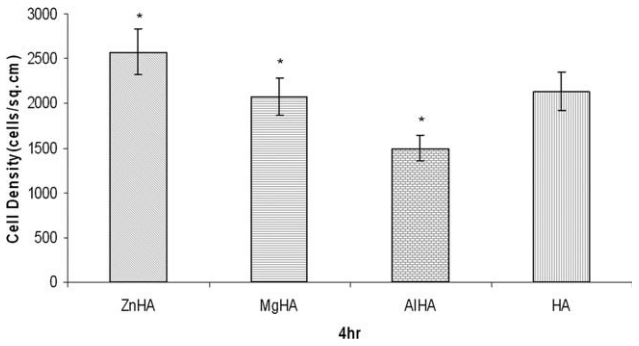

Figure 7. Osteoblast adhesion on 5% ZnHA, 5% MgHA, 5% AlHA, and HA-coated titanium substrates using RAMS. $*p < 0.1$ compared with RAMS HA-coated titanium substrates.

and the surrounding chemical and biological environment. More systematic studies would be needed to verify this.

Since the solubility of apatite is inversely related to its crystallinity, it was expected that all the doped coatings, being amorphous, would not endure a 4-day test. In the experiments, all three types of doped coatings dissolved very fast, and by the end of day 4 only a minimal amount of the coating still remained on the substrates. However, pure HA coatings only experienced limited dissolution. Therefore, a comparison of cell proliferation was not made. The stability of the HA coating (i.e., resistance to dissolution) is crucial in the early stage of the bone mineralization process. If the HA coating dissolves too rapidly *in vivo*, osteoblast contact with the implant surface is likely to be reduced. In contrast, an excessively crystalline coating will inhibit cell proliferation. Therefore, partially crystalline HA may be the most desirable coating to encourage cell attachment, because it is degradable and can stimulate bone in-growth as it dissolves gradually in the physiological environment.

To determine the cell viability after seeding onto different substrates, the cultures were incubated with calcein-AM and ethidium homodimer at a concentration of 2 μM for 10 min and monitored under a fluorescence microscope at each stage of cell culture. Figure 8 shows the green fluorescence

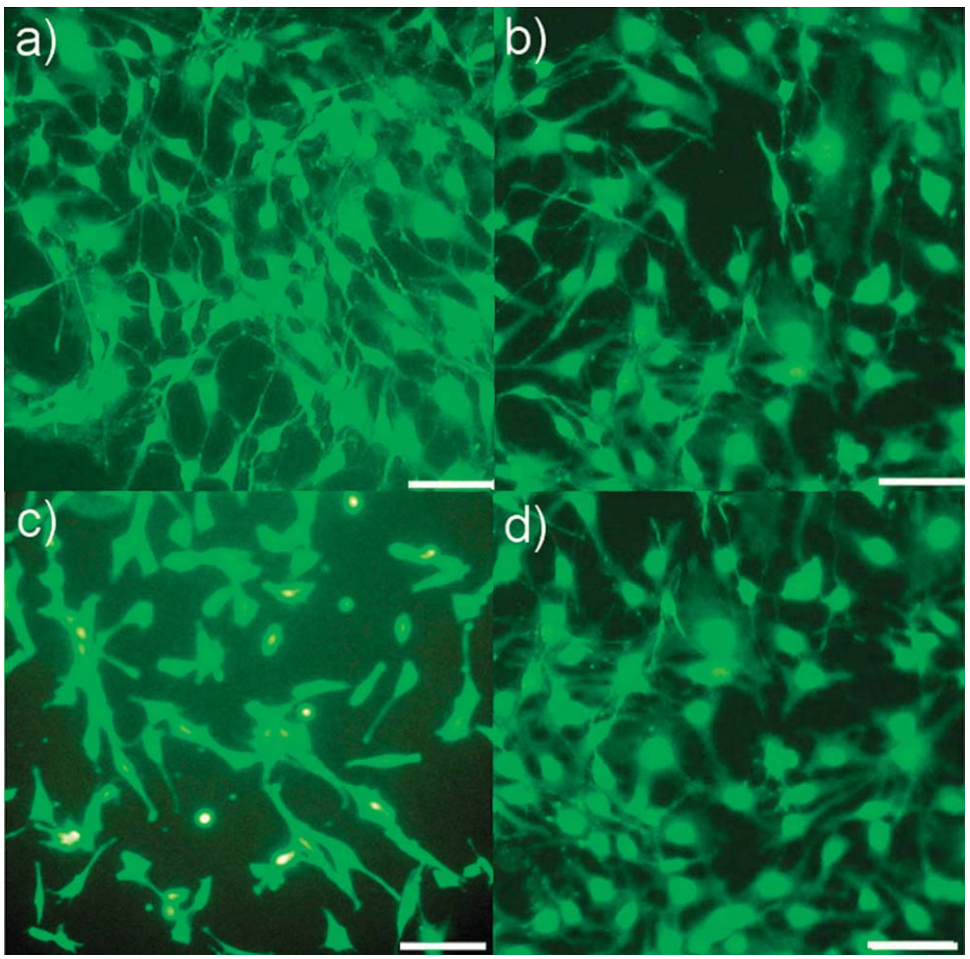

Figure 8. Osteoblast proliferation on titanium substrates coated with (a) 5% ZnHA, (b) 5% MgHA, (c) 5% AlHA, and HA using RAMS 4 days after seeding. Scale bars show 50 μm. [Color figure can be viewed in the online issue, which is available at www.interscience.wiley.com.]

observed when the living cells were incubated with calcein-AM. In contrast, ethidium homodimer penetrates dead/permeable cells and gives a red fluorescence. In our experiments we found the red fluorescence (not shown) was negligible, suggesting that most of the attached cells were healthy and evolved continuously.

The cell numbers on each substrate were consistent with those during the initial adhesion stage, except for 5%AlHA, which decreased cell density after normalization to adhesion. In some area of ZnHA coatings the local cell density was high enough to agglomerate.

CONCLUSIONS

It has been shown that RAMS HA and HA-related coatings can produce stoichiometric, thin, nanocrystalline HA coatings without the need for *in-situ* or *ex-situ* annealing. *In vitro* cell culture studies have demonstrated that osteoblast adhesion and proliferation significantly improves on RAMS HA coatings compared to plain substrates. Future investigations of the RAMS process should address: i) the importance of low crystallinity for HA-related coatings, ii) long-term osteoblast/osteoclast proliferation, iii) the effect of coatings on cell differentiation, and iv) *in vivo* clinical trials. In summary, the results presented here indicate that further studies on RAMS HA coatings have the potential to enhance various biomedical applications.

References

1. Lemons JE. Hydroxyapatite coatings. Clin Orthop Relat Res 1988;235:220–223.
2. Cooke FW. Ceramics in orthopedic surgery: Hip and knee implant fixation and wear. Clin Orthop Relat Res 1992; 276:135–146.
3. Bauer TW, Geesink RCT, Zimmerman R, McMahon JT. Hydroxyapatite-coated femoral stems. Histological analysis of components retrieved at autopsy. J Bone Surg A 1991;73:1439–1452.
4. Collier JP, Surprenant VA, Mayor MB, Wrona M, Jensen RE, Surprenant HP. Loss of hydroxyapatite coating on retrieved, total hip components. J Arthroplast 1993;8:389–393.
5. LeGeros RZ. Biodegradation and bioresorption of calcium phosphate ceramics. Clin Mater 1993;14:65–88.
6. Xu JL, Khor KA, Gu YW, Kumar R, Cheang P. Radio frequency (rf) plasma spheroidized HA powders: Powder characterization and spark plasma sintering behavior. Biomaterials 2005;26:2197–2207.
7. Filiaggi MJ, Coombs NA, Pilliar RM. Characterization of the interface in the plasma-sprayed HA coating/Ti-6Al-4V implant system. J Biomed Mater Res 1991;25:1211–1229.
8. Jansen JA, Wolke JGC, Swann S, van der Waerden JP, de Groot K. Application of magnetron sputtering for producing ceramic coatings on implant materials. Clin Oral Implant Res 1993;4:28–34.
9. Hulshoff JEG, van Dijk K, van der Waerden JP, Wolke JGC, Ginsel LA, Jansen JA. Biological evaluation of the effect of magnetron sputtered Ca/P coatings on osteoblast-like cells in vitro. J Biomed Mater Res 1995;29:967–975.
10. van Dijk K, Schaeken HG, Wolke JGC, Jansen JA. Influence of annealing temperature on RF magnetron sputtered calcium phosphate coatings. Biomaterials 1996;17:405–410.
11. Ong JL, Lucas LC. Post-deposition heat treatments for ion beam sputter deposited calcium phosphate coatings. Biomaterials 1994;15:337–341.
12. Yamashita K, Arashi T, Kitagaki K, Yamada S, Umegaki T. Preparation of apatite thin films through rf-sputtering from calcium phosphate glasses. J Am Ceram Soc 1994;77:2401–2407.
13. Yang Y, Kim K, Agrawal CM, Ong JL. Effect of post-deposition heating temperature and the presence of water vapor during heat treatment on crystallinity of calcium phosphate coatings. Biomaterials 2003;24:5131–5137.
14. Yang Y, Kim KH, Agrawal CM, Ong JL. Influence of post-deposition heating time and the presence of water vapor on sputter-coated calcium phosphate crystallinity. J Dent Res 2003;82:833–837.
15. Thian ES, Huang J, Best SM, Barber ZH, Bonfield W. Magnetron co-sputtered silicon-containing hydroxyapatite thin films–An *in-vitro* study. Biomaterials 2005;26:2947–2956.
16. Wolke JGC, deGroot K, Jansen JA. In vivo dissolution behavior of various RF magnetron sputtered Ca-P coatings. J Biomed Mater Res 1998;39:524–530.
17. Nelea V, Morosanu C, Iliescu M, Mihailescu IN. Hydroxyapatite thin films grown by pulsed laser deposition and radio-frequency magnetron sputtering: comparative study. Appl Surf Sci 2004;228:346–356.
18. Okamoto K, Matsuura T, Hosokawa R, Akagawa Y. RGD peptides regulate the specific adhesion scheme of osteoblasts to hydroxyapatite but not to titanium. J Dent Res 1998;77: 481–487.
19. Sato M, Slamovicha EB, Webster TJ. Enhanced osteoblast adhesion on hydrothermally treated hydroxyapatite/titania/poly(lactide-co-glycolide) sol-gel titanium coatings. Biomaterials 2005;26:1349–1357.
20. Perozzollo D, Lacefiled WR, Brunette DM. Interaction between topography and coating in the formation of bone nodules in culture for hydroxyapatite- and titanium-coated micromachine surface. J Biomed Mater Res 2001;56:494–503.
21. Shu R, McMullen R, Baumann MJ, McCabel LR. Hydroxyapatite accelerates differentiation and suppresses growth of MC3T3-E1 osteoblasts. J Biomed Mater Res A 2003;67:1196–1204.
22. Zhu X, Eibl O, Berthold C, Scheideler L, Gerstorfer JG. Structural characterization of nanocrystalline hydroxyapatite and adhesion of preosteoblast cells. Nanotechnology 2006;17: 2711–2721.
23. Chou L, Marek B, Wagner WR. Effects of hydroxyapatite coating crystallinity on biosolubility, cell attachment efficiency and proliferation in vitro. Biomaterials 1999;20:977–985.
24. Balasundaram G, Sato M, Webster TJ. Using hydroxyapatite nanoparticles and decreased crystallinity to promote osteoblast adhesion similar to functionalizing with RGD. Biomaterials 2006;27:2798–2805.
25. Kilpadi KL, Chang PL, Bellis SL. Hydroxyapatite binds more serum proteins, purified integrins, and osteoblast precursor cells than titanium or steel. J Biomed Mater Res 2001;57:258–267.
26. Sawyera AA, Hennessyb KM, Bellis SL. Regulation of mesenchymal stem cell attachment and spreading on hydroxyapatite by RGD peptides and adsorbed serum proteins. Biomaterials 2005;26:1467–1475.
27. Baxter LC, Frauchiger V, Textor M, Gwynn I, Richards RG. Fibroblast and osteoblast adhesion and morphology on calcium phosphate surfaces. Eur Cells Mater 2002;4:1–17.

28. Yliheikkila PK, Masuda T, Ambrose WW, Suggs CA, Felton DA, Cooper LF. Preliminary comparison of mineralizing multilayer cultures formed by primary fetal bovine mandibular osteoblasts grown on titanium, hydroxyapatite, and glass substrates. Int J Oral Maxillofac Implants 1996; 11:456–465.
29. Lavos ICV, Wolynec S, Deboni MC, Konig B. In vitro and in vivo biocompatibility testing of Ti-6Al-7Nb alloy with and without plasma-sprayed hydroxyapatite coating. J Biomed Mater Res 2001;58:727–733.
30. Hu Q, Zhou T, Liu Y, Tao J, Cai Y, Zhang M, Pan H, Xu X, Tang R. Effect of crystallinity of calcium phosphate nanoparticles on adhesion, proliferation, and differentiation of bone marrow mesenchymal stem cells. J Mater Chem 2007;17:4690–4698.
31. Hong Z, Luan L, Paik SB, Deng B, Ellis DE, Ketterson JB, Mello A, Eon JG, Terra J, Rossi A. Crystalline hydroxyapatite thin films produced at room temperature: An opposing radio frequency magnetron sputtering approach. Thin Solid Films 2007;515:6773–6780.
32. Mello A, Hong Z, Rossi AM, Luan L, Querido W, Eon J, Terra J, Balasundaram G, Webster J, Feinerman A, Ellis DE, Ketterson JB, Ferreira CL. Osteoblast proliferation on hydroxyapatite thin coatings produced by right angle magnetron sputtering. Biomed Mater 2007;2:67–77.
33. Dumbleton J, Manley MT. Hydroxyapatite-coated preostheses in total hip and knee arthroplasty. J Bone Joint Surg Am A 2004;86:2526–2540.
34. Nounah A, Szilagyi J, Lacout JL. La substitution calcium-cadmium dans les hydroxyapatites. Ann Chim France 1990; 15:409–419.
35. Hong Z. Characterization of hydroxyapatite thin films prepared by right angle magnetron sputtering for biomedical applications. Doctorate Thesis, Illinois: Northwestern University; 2007.
36. Ito A, Ojima K, Naito H, Ichinose N, Tateishi T. Preparation, solubility, and cytocompatibility of zinc-releasing calcium phosphate ceramics. J Biomed Mater Res 2000;50:178–183.